Steam reforming of the bio-oil aqueous fraction in a fluidized bed reactor with *in-situ* CO_2 capture

Aingeru Remiro*, Beatriz Valle, Borja Aramburu, Andrés T. Aguayo, Javier Bilbao, Ana G. Gayubo

Chemical Engineering Department, University of the Basque Country

*P. O. Box 644, 48080, Bilbao, Spain. Phone: +34 946015361. Fax: +34 946013500. *Email: aingeru.remiro@ehu.es*

Abstract

The effect of CO_2 capture in the hydrogen production by steam reforming of the bio-oil aqueous fraction was studied. The reforming and cracking activity of the adsorbent (dolomite) and relationship between these reactions and those corresponding to the catalyst (reforming and WGS) were considered. The experiments were conducted in a two-step system with first step at 300 ºC for pyrolytic lignin retention. The remaining volatiles were reformed in a subsequent fluidized bed reactor on a Ni/La_2O_3-αAl_2O_3 catalyst. A suitable balance was stricken between reforming and WGS reactions, on the one side, and cracking and coke formation reactions, on the other side, at 600 ºC for catalyst/dolomite mass ratios ≥ 0.17. At this temperature and space-time of 0.45 $g_{catalyst}$ h $(g_{bio\text{-}oil})^{-1}$, bio-oil was fully converted and the H_2 yield was around 99 % throughout the CO_2 capture step. Catalyst deactivation was very low because the cracking hydrocarbon products (coke precursors) are reformed.

Keywords: Steam reforming, Bio-oil, Hydrogen, Deactivation, Ni/La_2O_3-αAl_2O_3 catalyst, CO_2 capture, Dolomite

1. Introduction

Bio-oil is considered a suitable raw material for the sustainable production of hydrogen, in order to satisfy its growing demand as a fuel and petrochemical raw material (for ammonia and methanol production). Besides, the use of hydrogen in processes of petroleum hydrotreatment and in agriculture, food and metallurgical industries[1-3] also contributes to increasing its current demand. Bio-oil production by flash pyrolysis of lignocellulosic biomass is an attractive way for valorizing a renewable material of diverse nature (and geographically delocalized), given that it is an environmentally friendly process without net CO_2 emission. In addition, the pyrolysis can be performed with simple technologies with a high level of technological development and thereby, a reasonable infrastructure investment is required.[4-6]

The bio-oil is a complex mixture of different families of oxygenate compounds with a high water content (around 21-27 wt % in the bio-oil obtained from wood and 39-51 wt % in that obtained from herbs).[7-10] This high water content boosts the interest of its valorization by steam reforming, avoiding the costly separation of water needed for its valorization as a fuel.[11,12] In recent bibliographic reviews, many studies on the reforming of raw bio-oil or its aqueous phase are reported.[13,14] The bio-oil aqueous fraction is obtained by phase separation after adding water to raw bio-oil.[15] This aqueous phase is less interesting than the organic fraction (insoluble in water) for certain bio-oil applications, such as: extraction of valuable compounds[16] (phenols, organic acids, levoglucosane and hydroxyacetaldehyde); use as a fuel[17,18] and co-feeding in refinery units such as FCC.[19-22] However, catalytic reforming of the bio-oil aqueous fraction means fewer problems than reforming raw bio-oil, given that the lower content of phenols (coming from the pyrolysis of biomass lignin), which show a higher influence on the coke formation on the catalyst.[23]

The technological development for bio-oil steam reforming faces the challenge of protecting the catalyst from coke deposition, with the most significant cause being the repolymerization (as pyrolytic lignin) of the bio-oil compounds derived from the pyrolysis of biomass lignin. In the literature, several strategies have been used aimed at preventing coke deposition: i) raw bio-oil aging by prior thermal treatment, which causes the pyrolytic lignin deposition[24]; ii) co-feeding of bio-oil and methanol into the reactor[25]; iii) two-step operation for the removal of pyrolytic lignin in the first step (thermal or with a low-cost catalyst), so that the remaining volatiles are reformed in a subsequent catalytic reactor.[26-28]

The development of reforming catalysts has been based on many studies about the steam reforming of certain bio-oil constituent compounds (acetic acid, acetone, phenol,

acetol, etc.). In these papers, Ni based catalysts (promoted with La, Co, Mg and Cu)[29-35] and supported noble metals[36,37] were used. The Ni based catalysts are commonly used for bio-oil reforming due to their good balance concerning activity, stability and cost.[38-42]

The fluidized bed reactor provides significant advantages for catalytic steam reforming of bio-oil [38-41,43]: i) isothermicity, which is an important point for an endothermic reaction; ii) low catalyst deactivation, due to a homogeneous deposition of pyrolytic lignin on the catalyst[44]; iii) simple scaling up and iv) capability for *in situ* utilization of CO_2 solid adsorbent, in order to shift the thermodynamic equilibrium of reforming reaction.

The stoichiometry of the bio-oil aqueous fraction reforming reaction is:

$$C_nH_mO_k + (n\text{-}k)H_2O \rightarrow nCO + \left(n + \frac{m}{2} - k\right)H_2 \quad (1)$$

This reaction is followed by the water-gas-shift reaction (WGS):

$$CO + H_2O \Leftrightarrow CO_2 + H_2 \quad (2)$$

Thus, the overall steam reforming can be represented as follows:

$$C_nH_mO_k + (2n\text{-}k)H_2O \rightarrow nCO_2 + \left(2n + \frac{m}{2} - k\right)H_2 \quad (3)$$

Additionally, there are secondary reactions:

Cracking: $C_nH_mO_k \rightarrow C_xH_yO_z$ + gas (H_2, CO, CO_2, CH_4,….) + coke (4)

Methane reforming: $CH_4 + H_2O \Leftrightarrow CO + 3\ H_2$ (5)

Boudouard reaction: $2\ CO \Leftrightarrow CO_2 + C$ (6)

In this paper, the steam reforming of bio-oil aqueous fraction has been studied on a Ni/La_2O_3-αAl_2O_3 catalyst in a fluidized bed reactor with *in situ* CO_2 capture. The kinetic behavior of the catalyst has been analyzed in previous studies on the reforming of bio-oil aqueous fraction (without capture), which were focused on establishing a suitable catalyst composition and studying the effect of La_2O_3 addition.[45] The effect of operating conditions (temperature, steam/carbon ratio, space velocity) on hydrogen yield and selectivity, and the coke formation mechanism on this catalyst have also been studied.[46]

The use of a CO_2 adsorbent in the reactor has already been studied for the bio-oil steam reforming in a fixed bed reactor.[47] Natural rocks, such as limestone and dolomite, have been widely used as adsorbents because of their availability and low cost. Dolomite has great mechanical resistance and high stability for operating in carbonation-calcination

cycles, because CaO sintering is attenuated by the presence of MgO.[48] The dolomite capacity for CO_2 capture is due to the CaO carbonation reaction:

$$CO_2 + CaO \Leftrightarrow CaCO_3 \quad (7)$$

This reaction is able to shift the thermodynamic equilibrium of the reactions involved in the bio-oil reforming (eq. 3), thus increasing the hydrogen yield.

The aim of this study is to establish the optimum conditions (catalyst/dolomite ratio and temperature) for the bio-oil aqueous fraction reforming with *in situ* CO_2 capture. Accordingly, the effect of reforming and cracking activity of dolomite on the reaction system (eqs 1-6) has been quantified, and the relationship between this activity and that of the catalyst has been considered.

2. Experimental

2.1. Bio-oil production and composition

The raw bio-oil was obtained by flash pyrolysis of pine sawdust at 480 ºC in a semi-industrial demonstration plant, located in Ikerlan-IK4 technology center (Alava, Spain), with a biomass feeding capacity of 25 kg/h.[49] This development of this plant was based on previous results obtained in a laboratory plant (120 g/h) at the University of the Basque Country.[50,51] The bio-oil aqueous fraction was obtained by phase separation after adding water to raw bio-oil, in water/bio-oil mass ratio= 2/1, following the procedure described by Czernik et al.[38] The raw bio-oil and its aqueous fraction composition were determined, in water-free basis, by GC/MS analyser (*Shimadzu QP2010S device*) and the results are shown in Table 1. The corresponding molecular formulas are $C_{4.3}H_{7.2}O_{2.6}$ and $C_{4.1}H_{7.4}O_{2.7}$, respectively. The water content, determined by Karl Fischer valorization (*KF Titrino Plus 870*), were 35 wt% in the raw bio-oil and 82 wt% in the aqueous fraction. The average molecular weight, quantified by Gel Permeation Chromatography (GPC) (*Waters 616*), was 886 g mol^{-1} for the raw bio-oil and 634 g mol^{-1} for the aqueous fraction.

Table 1

2.2. Catalyst and adsorbent

The Ni/La_2O_3-αAl_2O_3 catalyst was prepared with 10 wt% of Ni by using a previously described method,[45] which was established by Alberton et al.[52] The La_2O_3-αAl_2O_3 support (with 10 wt% of La_2O_3) was obtained by impregnation of α-Al_2O_3, under vacuum at 70 °C, with an aqueous solution of $La(NO_3)_3 \cdot 6H_2O$ (*Alfa Aesar, 99%*) and followed by drying at

100 °C for 24 h and calcination at 900 °C for 3 h. Subsequently, an impregnation with $Ni(NO_3)_2 \cdot 6H_2O$ and drying at 110 °C for 24 h were carried out, and the final catalyst was calcined at 700 °C for 3 h.

The physical properties of the catalyst, such as BET surface area (37.6 $m^2\ g^{-1}$), pore volume (0.145 $cm^3\ g^{-1}$) and average pore size (11.9 nm) were evaluated from the N_2 adsorption-desorption isotherms, obtained by using a *Micromeritics ASAP 2010C* analyzer. This device was also used for hydrogen chemisorption measurements for quantifying Ni dispersion and specific metallic surface, with the resulting values of 1.9 % and 12.4 $m^2\ g_{metal}^{-1}$, respectively. These catalytic properties were previously described in detail.[45]

The dolomite used in this paper was provided by *Calcinor S.A.* (Tolosa, Spain) and its physical properties are listed in Table 2. The dolomite was sieved (90-150 μm) and calcined at 800 °C for 2 h in order to obtain the active phase (CaO).

Table 2

The TPO (temperature programmed oxidation) analyses of the coke deposited on the deactivated catalyst were conducted by combustion with air in a *Setaram TG-DSC-11 Calorimeter* coupled with a mass spectrometer *Thermostar Balzers Instrument* for monitoring the signals corresponding to masses 18 (H_2O) and 44 (CO_2). The coke deposited on dolomite samples was analyzed by thermogravimetry (combustion with air) in a *TA Instruments Q5000 IR* thermobalance. For both solids, the experimental procedure consisted in: i) stabilizing the sample for 30 min under air flow at 75 ºC; ii) heating the sample at 7 ºC min^{-1} up to 750 ºC and keeping this temperature for 30 min.

2.3. Reaction system and operating conditions

The reaction equipment consists of two reactors in-line (Figure 1). The first reactor (thermal treatment of bio-oil at 300 ºC) retains a carbonaceous solid (pyrolytic lignin) formed by re-polymerization of certain bio-oil oxygenates. This reactor has enough volume so that the flow is not blocked in several hours (usually 4 h, although 10 h experiments have been performed with no apparent problems). It has been proven in experiments with different duration that the deposited lignin composition (66.5 wt% C, 4.9 wt% H and 28.6 wt% O) and its deposition rate (4.6 mg min^{-1}) are constant. After each experiment, the lignin is easily removed from the reactor walls and the low amount adhered is removed by combustion with air at 600 °C. In a previous paper, the composition and properties of pyrolytic lignin and the effect of temperature on this composition were studied in detail.[53]

The volatile compounds that leave this thermal step are subsequently transformed (by catalytic steam reforming) in a second unit (fluidized bed reactor). The controlled deposition of pyrolytic lignin in a specific thermal step, prior to the catalytic reactor, minimizes the operating problems caused by this deposition and attenuates the catalyst deactivation. This fact was previously verified for the catalytic conversion of raw bio-oil into hydrocarbons.[53-55]

Figure 1

The on-line analysis of the reforming products is carried out continuously (more representative and steady than discontinuous sampling) with a gas chromatograph (*Agilent Micro GC 3000*) provided with four modules for the analysis of the following: (1) permanent gases (O_2, H_2, CO, and CH_4) with 5A molecular sieve capillary column; (2) light oxygenates (C_{2-}), CO_2 and water, with Plot Q capillary column; (3) C_2-C_4 hydrocarbons, with alumina capillary column; (4) oxygenated compounds (C_{2+}) with Stabilwax type column. The mass balances, calculated from chromatographic analysis of the bio-oil and of the product stream leaving the reforming reactor, were closed at ≥ 95 wt% in all experiments.

The experimental two-unit system was operated at atmospheric pressure and the feeding rate (0.1 ml min^{-1}) of the bio-oil aqueous fraction was controlled by an injection pump *Harvard Apparatus 22.* The particle size of catalyst and dolomite (obtained by sieving) was 150-250 μm and 90-120 μm, respectively. An inert solid (CSi (carborundum), with 30-50 μm particle size) was also used in the reactor, in inert/(catalyst+dolomite) mass ratio = 1/1, in order to improve the hydrodynamic properties of the catalytic bed (consisting of catalyst and/or dolomite). The particle sizes of the three solids are suitable for bed hydrodynamics and for allowing their separation after reaction, required for their individual characterization. The hydrodynamic properties of the reactor, which determines the feed flow-rate, were established by cold hydrodynamic studies, ensuring the fluidization of the catalyst + dolomite + CSi bed. The bed attrition was found negligible, by comparing the mass of the spent catalyst + CSi bed with the initial mass of the bed. The coke deposited on the spent catalyst was considered for this quantification.

The catalyst was reduced at 700 ºC for 2 h, by using a H_2-He flow (5 vol % of H_2), prior to each reforming reaction. The reforming conditions were: thermal step, 300 ºC; catalytic steam reforming, 550-650 ºC; space-time = 0.45-1.35 $g_{catalyst}$ h $(g_{bio\text{-}oil})^{-1}$; space-velocity ($G_{C1}HSV$) = 2300-7600 h^{-1} (calculated in CH_4 equivalent units); steam-to-carbon ratio (steam/carbon molar ratio in bio-oil) at fluidized bed reactor inlet (S/C) = 10. This

ratio corresponds to the water in the aqueous fraction of bio-oil at the outlet of thermal treatment. This aqueous fraction is obtained by adding water to raw bio-oil to achieve phase separation. After the reforming reaction, the catalytic bed was swept with He for 30 minutes at the reaction temperature in order to desorb the possible reaction products that may have been retained and to homogenize the coke deposited. This procedure was performed with both the catalyst and the adsorbent prior to the analysis by TPO.

3. Results

The dolomite activity for bio-oil conversion and its influence on the reaction medium composition should be considered, as the reforming of bio-oil oxygenates and the CO_2 capture take place in the same reactor. Consequently, the reforming reactions on the catalyst are affected by the reactions occurring on the dolomite (Figure 2). The bio-oil steam reforming proceeds with high efficiency when the operating conditions are suitable for attaining total CO_2 capture and hydrocarbon compounds are fully reformed. Thus, by-product yields are minimized and the H_2 formation is enhanced.

Figure 2

3.1. Reaction indices

In order to quantify the results the following reaction indices were used:

Bio-oil conversion: $$X = \frac{F_{inlet} - F_{exit}}{F_{inlet}} \quad (8)$$

where F is the molar flow-rate of oxygenates at the inlet and outlet of the reforming reactor, referred to the C atoms contained in the bio-oil.

Hydrogen yield: $$Y_{H_2} = \frac{F_{H_2}}{F^{o}_{H_2}} 100 \quad (9)$$

where F_{H_2} is the molar flow-rate of H_2 in the product stream and $F^{o}_{H_2}$ is the stoichiometric maximum of the bio-oil fed to the reactor (full conversion in eq. (3)).

The yield of each C containing product (CO_2, CO, CH_4 and hydrocarbons, mainly ethane and ethylene):

$$Y_i = \frac{F_i}{F_{inlet}} 100 \quad (10)$$

where F_i is the molar flow-rate of each compound, and F_{inlet} is the molar flow-rate of the

bio-oil fed into the reactor, in C units.

The indices shown above were applied to the second step of the reaction system, i.e., to the fluidized bed reactor (with dolomite or catalyst). The bio-oil molar flow-rate at the catalytic reactor inlet (F_{inlet}) is indirectly determined by a mass balance in the thermal treatment step (at 300 °C). Accordingly, the amount of oxygenates from the bio-oil aqueous fraction ($C_{4.1}H_{7.4}O_{2.7}$) retained as pyrolytic lignin (in this thermal step) and its composition are determined after each experimental run. The average amount of pyrolytic lignin deposited is 25 (± 2) wt% (by mass unit of oxygenates contained in the bio-oil aqueous fraction) and its average composition is $C_{5.5}H_{4.9}O_{1.8}$ (quantified by elemental analysis). Consequently, the average composition of the treated bio-oil that enters the fluidized bed reforming reactor is $C_{3.6}H_{8.3}O_{3.0}$. The bio-oil molar flow-rate at reactor outlet (F_{outlet}) is calculated from the molar fraction of oxygenates (analyzed by microGC and by GC/MS) and the total number of moles at the reactor outlet, F_T, determined by elemental mass balance of H atoms in the catalytic reactor, Eq. (11), given that H atoms are not affected by CO_2 capture.

$$F_T = \frac{F_{H,inlet}}{\sum x_i \cdot n_{H,i}} \tag{11}$$

where $F_{H,inlet}$ is the flow-rate of H atoms at the reforming reactor inlet (indirectly calculated in each run by a mass balance applied to the thermal step, thus considering the H retained in the pyrolytic lignin); x_i is the molar fraction of each reaction product, and $n_{H,i}$ is the number of H atoms in each product of the outlet stream.

The mass balance shown in Figure 3 should be considered in order to obtain the values corresponding to the transformation of the bio-oil aqueous fraction fed into the two-step system. Given that pyrolytic lignin deposition in the thermal step involves separating 25 wt% of bio-oil oxygenates, bio-oil conversion and product yields (eqs 8-10) must be multiplied by 0.75 in order to refer these results to the bio-oil fed into the system. It should be noted that the mass balance closure corresponding to Figure 3 is ± 3%.

Figure 3

3.2. Activity of the dolomite

In order to understand the role of the dolomite used as CO_2 adsorbent in the complex reaction system (Figure 2), its activity was analyzed in experiments without catalyst in the reactor. The bed is composed of dolomite and CSi (inert). The experiments were performed

with the following conditions: 600 °C; S/C, 10; mass of dolomite, 3 g; bio-oil flow-rate, 0.1 cm^3 min^{-1}; time on stream, 3.5 h.

It should be noted that the dolomite is active for both the reforming of bio-oil compounds (Figure 4a) and their thermal cracking (Figure 4b). As mentioned above, certain bio-oil compounds (acetic acid and acetol) undergo thermal cracking on a sand bed under steam reforming conditions, with acetic acid being significantly converted into H_2, CO_2, CO, CH_4 and C_2 hydrocarbons.[34,56] Figure 4 shows that bio-oil conversion decreases with time on stream and so the H_2 yield also decreases (from 29 % to 20 % in 3.5 h). The dolomite keeps the capacity for CO_2 capture throughout 1.7 h (Figure 4a), and it then steadily loses this capacity.

Figure 4

In addition to H_2 and CO_2, other products from cracking and reforming of bio-oil oxygenates are obtained, such as CO, CH_4 and light hydrocarbons (mainly ethane, ethylene and propylene) (Figure 4b). The cracking significance is evidenced by the high CH_4 yield at zero time on stream (≈11 %), although the products selectivity changes with reaction time due to the dolomite deactivation. Thus, CH_4 yield decreases to 6 % in 3.5 h and the yields of CO and hydrocarbons increase (the former to a greater extent). It should be noted that CO formation becomes more noticeable when CO_2 capture capacity of the dolomite decreases (above 1.7 h, under the conditions studied).

The afore-mentioned results evidence the important role of the CO_2 adsorbent (by cracking and reforming reactions) in the bio-oil catalytic reforming reaction. Besides, contribution of thermal cracking reactions should also be considered. In order to quantify the significance of these thermal reactions in the bio-oil steam reforming, some experiments were carried out without dolomite (only inert CSi in the reactor). Figure 5 compares the results obtained with dolomite (reforming/cracking) and with CSi (thermal cracking) at zero time on stream in the 550-800 °C range. As temperature is increased the bio-oil conversion increases (up to 0.8 at 800 °C) and thermal cracking contributes significantly to this conversion above 600 °C (Figure 5a). The H_2 and CO_2 yields are also higher when temperature is increased above 600 ºC (up to 20 % at 800 ºC). Similarly, the yields of other thermal cracking products (CH_4 CO and HCs) also increase (Figure 5b) when is higher than 600 ºC. Based on the results in Figure 5, the presence of dolomite in the reactor gives way to a decrease by 50 °C in the temperature at which bio-oil conversion is noticeable, since the formation of H_2 and other reforming/cracking products is observed at 550 ºC. CO_2 formation is not significant below 600 °C because carbonation equilibrium

is favored. Moreover, the lower CO yield obtained with dolomite, compared to that obtained with CSi, is explained by the dolomite activity to the WGS reaction.

Figure 5

3.3. Suitable conditions for steam reforming with CO_2 capture

In this section, the main process conditions are analyzed by using a mixture of catalyst and dolomite in the fluidized bed reforming reactor.

3.3.1. Dynamics of bio-oil steam reforming with in situ capture of CO_2

Steam reforming with *in situ* CO_2 capture of the bio-oil aqueous fraction was studied under the following operating conditions: 600 ºC; $G_{C1}HSV$, 7200 h^{-1}; S/C, 10; space-time, 0.45 $g_{catalyst}$ $h(g_{bio\text{-}oil})^{-1}$; amount of dolomite, 1.3 g; catalyst/dolomite mass ratio, 0.17; time on stream, 4 h. The results of bio-oil conversion and product yields are shown in Figure 6, where the three successive steps corresponding to the CO_2 capture dynamics are distinguished: i) total capture; ii) breakthrough curve (gradual saturation of dolomite with CO_2); iii) total saturation of dolomite (steam reforming without CO_2 adsorption). In calcination experiments of saturated dolomite, conducted in a thermobalance, it was determined that CaO conversion during the carbonation in the reactor is 88% (± 1%).

Figure 6

In order to analyze these results it should be consider that the dolomite plays an active role in the cracking and reforming reactions of bio-oil compounds during these three steps (section 3.2). Under the reforming conditions used, the bio-oil is fully converted throughout 4 h reaction (Figure 6a). The period of almost total CO_2 capture lasts around 40 min and, during this time, the H_2 yield is over 99 % and it decreases slightly when the dolomite is fully saturated. The low yield of CH_4 is due to the catalyst activity for its reforming. Furthermore, the yield of hydrocarbons is very low under these reaction conditions. However, the presence of this kind of compounds in the reaction medium has a direct impact on the catalyst deactivation by coke deposition on its active sites.[46] Consequently, reaction conditions that minimize the concentration of these coke precursors in the reaction medium should be established.

Furthermore, in the period of almost total CO_2 capture (40 min) the CO yield is lower than 0.5 %, and it increases up to 5 % after dolomite saturation (Figure 6b). This result is explained because the WGS reaction (eq. 2) is shifted due to the CO_2 removal from the reaction medium, thereby minimizing the formation of CO. This fact is important in order

to lessen the severity of a subsequent treatment for H_2 purification (with the consequent economic advantage).

3.3.2. Effect of catalyst/dolomite mass ratio

This ratio should be studied because dolomite is active for bio-oil reforming and cracking, i.e., both catalyst and dolomite are active for the transformation of the reaction medium compounds. The experiments were carried out under the same operating conditions of section 3.3.1 and varying the catalyst/dolomite mass ratio in the 0.03 - 0.38 range. The catalyst mass was 0.5 g and a different mass of dolomite (1.3, 3.0, 5.0 and 15.0 g) was used in each experiment.

Figure 7 shows the effect of catalyst/dolomite mass ratio on the bio-oil conversion and product yields. The results correspond to zero time on stream (almost total CO_2 capture) and to 4 h of time on stream (there is no CO_2 capture for catalyst/dolomite mass ratios higher than 0.1, as the dolomite is saturated). It is observed that catalyst/dolomite mass ratios higher than 0.17 are required to achieve the stoichiometric yields of the reforming and WGS reaction. For these mass ratios the catalyst deactivation by coke deposition is minimized. Under these operating conditions, the initial results (0 h) correspond to a situation with total CO_2 capture and the results at 4 h correspond to a situation with no capture (for catalyst/dolomite mass ratios higher than 0.1).

Figure 7

The above-mentioned results evidence that minimum catalyst/dolomite ratio of around 0.17 is required in order to attain suitable results. Figure 8 shows the evolution with time on stream of bio-oil conversion (Figure 8a) and product yields (Figures 8b-f) for different catalyst/dolomite mass ratios (pointed lines) and for the reaction without dolomite (dashed line). This figure provides a more complete view of the effect of this ratio and the dolomite role.

Figure 8

For catalyst/dolomite ratios higher than or equal to ($\geq$) 0.17, the results of conversion and products yields are better than those obtained without dolomite (only catalyst in the reactor), with the bio-oil being fully converted (Figure 8a) and H_2 yields above 95 % throughout the reaction time (Figure 8b).

In order to explain the results, differences between the periods of total CO_2 capture (the first 40 min) and when the dolomite is not active for this capture should be considered.

In the initial period of nearly total capture, the CO_2 yield is ≈ 5 % (corresponding to the thermodynamic equilibrium of CaO carbonation in dolomite (eq 7) at 600 °C, Figure 8c), being negligible the yield of CO (Figure 8d) for catalyst/dolomite mass ratios ≥ 0.17. This result reveals that the WGS reaction is completely shifted. Besides, CH_4 and light hydrocarbons, which are products of the bio-oil compounds cracking, are almost fully reformed (Figures 8e,f). Therefore, the development of these compounds to more condensed structures (coke precursors) is avoided, and so the catalyst deactivation in 4 h reaction is negligible.

In the period of dolomite saturation (from 40 min to 2 h) and after its total saturation (above 2h, Figure 6), the dolomite capacity for reforming and cracking the bio-oil compounds (section 3.2) should be considered. For catalyst/dolomite mass ratios ≥ 0.17, the CO and CO_2 yields increase with time on stream (Figures 8c,d) and the yields of CH_4 (Figure 8e) and hydrocarbons (Figure 8f) are negligible. The bio-oil conversion (Figure 8a) and H_2 yield (Figure 8b) keep almost constant thorough reaction time due to the dolomite activity for reforming and cracking (to a lesser extent) the bio-oil oxygenates, which forms lighter oxygenates and hydrocarbons liable to reforming. Thus, bio-oil heavy compounds, which are presumably more active precursors in coke formation, are cracked. Therefore, combining the dolomite and catalyst cracking/reforming capacities (for catalyst/dolomite ≥ 0.17), the main by-products obtained thorough the dolomite saturation period are CO_2 and CO (due to the WGS reaction equilibrium).

The results in Figure 8 also reveal that catalyst/dolomite mass ratios lower than 0.17 are not suitable because the catalyst amount is not enough to reform the cracking products coming from the dolomite. Consequently, the bio-oil conversion (Figure 8a) and H_2 yield (Figure 8b) decrease more rapidly with time on stream than without dolomite (catalyst alone), and a high yield of CH_4 (≈ 16%) is obtained at zero time on stream (Figure 8e), which decreases slightly to 12 % in 4 h reaction. The decrease in CH_4 yield is related to the decrease of dolomite cracking capability as a result of carbonation (also evidenced in Figure 4). However, the CH_4 yield decrease is less pronounced than the decrease in bio-oil conversion, as a result of the loss of CH_4 reforming capacity of the catalyst due to deactivation. Besides, the initial yield of hydrocarbons is negligible and it increases with time on stream (Figure 8f) due to the catalyst deactivation, which causes the loss of reforming activity.

3.3.3. Effect of the amounts of dolomite and catalyst

The experiments were performed by using different amounts of dolomite (1.3 and 3.9 g) and catalyst (0.5 and 1.5 g) in order to have a constant catalyst/dolomite ratio (0.38). The other operating conditions are the same as those used in section 3.3.1. The results corresponding to the evolution with time on stream of H_2 and CO_2 yields (Figure 9a) and CO and CH_4 yields (Figure 9b) are shown.

Figure 9

It should be noted that for both masses studied the yields of CO_2, CO and CH_4 are almost negligible during the period of total CO_2 capture. Then, the CO_2 and CO yields increase throughout the period in which dolomite loses its capture capability, with their final yields being similar for both conditions.

The afore-mentioned results evidence that the process of CO_2 capture, under the operating conditions studied, is greatly influenced by: i) the catalyst amount, established to achieve full conversion of the bio-oil fed during the time desired (which is higher as the catalyst mass in the bed is increased) and ii) the catalyst/dolomite mass ratio (which should be ≥ 0.17).

3.3.4. Effect of reforming temperature

Thermodynamics and kinetics of all reactions involved in the process (reforming, WGS, dolomite carbonation and secondary cracking reactions, Figure 2) are affected by the reaction temperature. This effect was studied in the 550-650 °C range because the catalyst deactivation by coke is very high at temperatures below 550 °C (as proven in a previous paper without CO_2 capture[46]), and above 650 ºC the capture of CO_2 is thermodynamically unfavored.[57] The operating conditions were: 3 g of dolomite, catalyst/dolomite ratio = 0.17, S/C = 10, 0.45 $g_{catalyst}$ h $(g_{bio\text{-}oil})^{-1}$ and space-velocity ($G_{C1}HSV$) = 6900-7600 h^{-1}.

Figure 10 shows the effect of temperature on the evolution of bio-oil conversion (Figure 10a) and reaction products (Figures 10b-f) with time on stream. The catalyst deactivation and dolomite carbonation capacity are greatly affected by reaction temperature. The initial CO_2 capture (fresh dolomite) at 550 °C is almost total (Figure 10c) and bio-oil conversion and H_2 yield decrease notably with time on stream, due to the significant deactivation by coke deposition undergoing the catalyst at this temperature. At 650 °C, the initial CO_2 capture is not total (Figure 10c), which evidences that the thermodynamic equilibrium of reforming reaction is not completely shifted. The yield of CO steadily increases with time on stream due to the WGS reaction equilibrium. It should be noted that hydrocarbons are formed at 650 ºC, mainly CH_4 (Figure 10e) and light

hydrocarbons (Figure 10f). These hydrocarbon products come from the cracking reactions undergone by bio-oil compounds, which are promoted by the presence of dolomite at this temperature (Figure 5). Consequently, the H_2 yield at 650 ºC is lower than that obtained at 600 °C.

Figure 10

Figure 11 shows the temperature-programmed-oxidation (TPO) results of the coke deposited on the catalyst deactivated at different reforming temperatures (Figure 11a) and on the deactivated dolomite (Figure 11b). The results of coke content on the catalyst are consistent with the effect of temperature on decreasing the bio-oil conversion with time on stream (Figure 10), with these coke contents being 2.31 wt%, 0.56 wt% and 0.54 wt% at 550 ºC, 600 ºC and 650 ºC, respectively. Furthermore, the number of peaks in the TPO curves and the corresponding temperature provide information about the existence of different coke fractions, with different composition and growth level towards graphitic structures.[58-61] The position of TPO combustion peaks in supported metal catalysts and bi-functional catalysts is related to the proximity between the metal and the coke and to the metal ability to activate coke combustion.[59-60] The TPO results in Figure 11a show three peaks with maxima at 285 ºC, 420-445 ºC and 630-660 ºC, respectively, which are attributed to the combustion of the coke deposited on Ni atoms, Ni-La_2O_3 and Ni-Al_2O_3 interface and α-Al_2O_3 support, respectively.

The effect of reaction temperature on the TPO results is significant due to the increase in temperature promoting coke gasification. Therefore, although gasification seems to affect all coke types, the interpretation of these TPO results under these conditions of partial gasification of the coke is a difficult task.

The TPO results for the coke deposited on the dolomite used at different reforming temperatures (Figure 11b) are masked by those for CO_2 formation above 500 ºC due to the dolomite decarbonation. This fact makes impossible to determine the presence of coke fractions burning above 500 ºC. The content of the coke that burns below 500 °C is low (0.75 wt% and 0.48 wt% for reforming runs at 550 °C and 650 °C, respectively) but the TPO peak position (below 400 °C) suggests that this coke is deposited on the metallic sites of the dolomite (0.3 wt% Fe_2O_3, Table 2). This evidences that, as previously found,[62] these metallic sites are active for reforming reactions. The coke content deposited on the dolomite is lower than that corresponding to the catalyst, but it is presumably enough to deactivate the metallic sites of the dolomite.

Figure 11

According to the afore-mentioned results, 600 °C is a suitable temperature for the bio-oil aqueous fraction reforming with *in situ* CO_2 capture by using dolomite as adsorbent, because bio-oil is fully converted throughout 4 h reaction and H_2 yield around 99 % (≈ 70 % if calculated with respect to the bio-oil fed into the two-unit system) is obtained. Moreover, this temperature is close to that required to attain the maximum carbonation capacity (625 °C for dolomite).[57] In addition, this moderate temperature allows reducing the energy requirement of the process and enhances the Ni based catalyst stability.

It should be noted that this result is achieved because the first thermal step (of pyrolytic lignin removal) allow separating the bio-oil heavier compounds, which would require higher temperatures for reforming. The compounds derived from the cracking of these heavy oxygenates would also require higher temperatures. Accordingly, the results of the technology with two reaction steps are promising for further studies aimed at scaling up.

3.3.5. Effect of S/C ratio

The results shown in the previous sections correspond to a feed of bio-oil aqueous fraction (82 wt% water) for which the S/C ratio at the reforming reactor inlet is of around 10. The effect of increasing the S/C ratio (to S/C = 15) was studied at 600 °C (Figure 12).

Figure 12

The results show that the values of product yields and the effect of CO_2 capture at zero time on stream and its evolution with time on stream are similar for both S/C ratios. For S/C = 15 there is a slight decrease in the CO yield (the WGS reaction is favored), although it is not enough to significantly effect the H_2 yield. Besides, this minor advantage is counterbalanced by the higher cost of energy for feed vaporization, and therefore an increase in S/C ratio over that corresponding to the bio-oil aqueous fraction is not advisable.

The results obtained with CO_2 capture are interesting for future scale-up studies, considering that both catalyst and adsorbent (after their separation) must be regenerated in fluidized bed reactors interconnected with the reforming unit. Therefore, the residence time of the solids in the reforming reactor must be suitable to achieve the objectives of a constant H_2 production and CO_2 capture throughout time. Furthermore, although the catalyst can be regenerated by coke combustion, fully recovering its activity, the irreversible deactivation that undergoes the dolomite (and calcite and other minerals) in carbonation-calcination cycles, is a design challenge of the process. In order to

implementing these reforming-regeneration strategies, the concepts proposed for the CH_4 reforming with CO_2 capture[63] could be used.

Conclusions

The understanding of the bio-oil aqueous fraction reforming requires to consider the linkage between all reactions involved in both the reforming and the cracking reactions of bio-oil oxygenates. Dolomite may reform the bio-oil above 550 °C, and this capacity is affected by deactivation. Moreover, as dolomite activity for reforming and WGS reactions decreases, the cracking reactions of bio-oil oxygenates (on this dolomite) become more significant, and therefore CH_4 and CO formation is enhanced.

The use of dolomite *in situ* in the fluidized bed reactor is effective for CO_2 capture, and therefore enhances the reforming reaction. Furthermore, the catalyst/dolomite mass ratio is relevant because both catalyst and dolomite are active for reforming and cracking, i.e., the presence of dolomite influences the kinetic behavior of the catalyst. At 600 °C and catalyst/dolomite mass ratios higher than or equal to 0.17, a suitable balance is stricken between the reforming and WGS reactions and the cracking and coke formation reactions. Accordingly, at 600 °C and a space-time of 0.45 $g_{catalyst}$ h $(g_{bio\text{-}oil})^{-1}$, the bio-oil is fully converted and the H_2 yield is around 99 % throughout the CO_2 capture step and around 95 % when dolomite is saturated. During the period of CO_2 capture, the yield of CO is around 0.5 %, which evidences that the WGS reaction equilibrium is effectively shifted. The CO yield increases to 5 % once dolomite has been fully saturated. Furthermore, the catalyst deactivation is very low because hydrocarbon compounds (coming from cracking), which are coke precursors, are fully reformed so that CO is the only significant by-product.

The reaction indices studied (conversion and product yields) are not directly influenced by the amount of dolomite, although it affects the saturation time. Consequently, the amount of catalyst to be used in the reactor is determined by the catalyst/dolomite mass ratio and the bio-oil flow-rate in the feed.

The results of this paper are interesting to establish the suitable operating conditions in a fluidized bed of a larger scale, with circulating catalyst and adsorbent.

Acknowledgments

This work was carried out with the financial support of the Department of Education Universities and Investigation of the Basque Government (IT748-13), of the University of the Basque Country (UFI 11/39) and of the Ministry of Science and Innovation of the Spanish Government (Project CTQ2012-13428/PPQ).

References

(1) Konieczny, A.; Mondal. K.; Wiltowski, T.; Dydo, P. Catalyst development for thermocatalytic decomposition of methane to hydrogen. *Int. J. Hydrogen Energy* **2008,** *33*, 264-272.

(2) Demirbas, A. Global renewable energy projections. *Energy Sources Part B* **2009**, *4*, 212-224.

(3) Kirtay, E. Recent advances in production of hydrogen from biomass. *Energy Conver. Manage.* **2011**, *52*, 1778-1789.

(4) Butler, E.; Devlin, G.; Meier, D.; McDonnell, K. A review of recent laboratory research and commercial developments in fast pyrolysis and upgrading. *Renew. Sust. Energy Re*v. **2011**, *15*, 4171-4186.

(5) Bridgwater, A.V. Review of fast pyrolysis of biomass and product upgrading. *Biomass Bioenergy* **2012***, 38*, 68-94.

(6) Meier, D.; van de Beld, B.; Bridgwater, A.V.; Elliott, D.C.; Oasmaa, A.; Preto, F. State-of-the-art of fast pyrolysis in IEA bioenergy member countries. *Renew. Sust. Energy Rev.* **2013**, *20*, 619-641.

(7) Czernik, S.; Bridgwater, A.V. Overview of applications of biomass fast pyrolysis oil. *Energy Fuels* **2004**, *18*, 590-598.

(8) Mohan, D.; Pittman, C.U.; Steele, P.H. Pyrolysis of wood/biomass for bio-oil: A critical review. *Energy Fuels* **2006**, *20*, 848-849.

(9) García-Perez, M.; Chaala, A.; Pakdel, H.; Kretschmer, D.; Roy, C. Characterization of bio-oils in chemical families. *Biomass Bioenergy* **2007**, *31*, 222-242.

(10) Mullen, C.A.; Strahan G.D.; Boateng A.A. Characterization of Various Fast-Pyrolysis Bio-Oils by NMR Spectroscopy. *Energy Fuels* **2009**, *23*, 2707-2718.

(11) García, L.; French, R.; Czernik, S.; Chornet, E. Catalytic steam reforming of bio-oils for the production of hydrogen: Effects of catalyst composition. *Appl. Catal. A: General* **2000**, *201*, 225-239.

(12) Czernik, S.; French, R.; Feik, C.; Chornet, E. Hydrogen by catalytic steam reforming of liquid byproducts from biomass thermoconversion processes. *Ind. Eng. Chem. Res.* **2002**, *41*, 4209-4215.

(13) Lemonidou, A.A.; Kechagiopoulos, P.; Heracleous, E.; Voutetakis, S. Steam reforming of bio-oils to hydrogen in *The Role of Catalysis for the Sustainable Production of Biofuels and Bio-chemicals*; Elsevier: Amsterdam, Netherlands, 2013.

(14) Trane, R.; Dahl, S.; Skjøth-Rasmussen, M.S.; Jensen, A.D. Catalytic steam reforming of bio-oil. *Int. J. Hydrogen Energy* **2012**, *37*, 6447-6472.

(15) Oasmaa, A.; Czernik, S. Fuel oil quality of biomass pyrolysis oils-state of the art for end users. *Energy Fuels* **1999**, *13*, 914-921.

(16) Effendi, A.; Gerhauser, H.; Bridgwater, A.V. Production of renewable phenolic resins by thermochemical conversion of biomass: A review. *Renew. Sust. Energy Rev.* **2008***, 12*, 2092-2116.

(17) García-Pérez, M.; Adams, T.T.; Goodrum, J.W.; Geller, D.P.; Das, K.C. Production and fuel properties of pine chip Bio-oil/Biodiesel blends. *Energy Fuels* **2007***, 21*, 2363-2372.

(18) Jiang, X.; Ellis, N. Upgrading Bio-oil through Emulsification with Biodiesel: Thermal Stability. *Energy Fuels* **2010**, *24*, 2699-2706.

(19) Corma, A.; Huber, G.W.; Sauvanaud, L.; O´Connor, P. Processing biomass-derived oxygenates in the oil refinery: Catalytic cracking (FCC) reaction pathways and role of catalyst. *J. Catal.* **2007***, 247*, 307-327.

(20) Domine, M.E.; Iojoiu, E.E.; Davidian, T.; Guilhaume, N.; Mirodatos, C. Hydrogen production from biomass-derived oil over monolithic Pt- and Rh-based catalysts using steam reforming and sequential cracking processes. *Catal. Today* **2008**, *133-135*, 565-573.

(21) Lappas, A.A.; Bezergianni, S.; Vasalos, I.A. Production of biofuels via co-processing in conventional refining processes. *Catal. Today* **2009***, 145*, 55-62.

(22) Bertero, M.; Sedran, U. Conversion of pine sawdust bio-oil (raw and thermally processed) over equilibrium FCC catalysts. *Bioresour. Technol.* **2013**, *135*, 644-651.

(23) Gayubo, A.G.; Aguayo, A.T.; Atutxa, A.; Valle, B.; Bilbao, J. Undesired components in the transformation of biomass pyrolysis-oil into hydrocarbons on a HZSM-5 zeolite. *J. Chem. Tech. Biotechnol.* **2005***, 80*, 1244-1251.

(24) Bertero, M.; de la Puente, G.; Sedran, U. Effect of pyrolysis temperature and thermal conditioning on the coke-forming potential of bio-oils. *Energy Fuels* **2011***, 25*, 1267-1275.

(25) Czernik, S.; Evans, R.; French, R. Hydrogen from biomass-production by steam reforming of biomass pyrolysis oil. *Catal. Today* **2007**, *129*, 265-268.

(26) Wang, Z.; Pan, Y.; Dong, T.; Zhu, X.; Kan, T.; Yuan, L.; Torimoto, Y.; Sadakata, M.; Li, Q. Production of hydrogen from catalytic steam reforming of bio-oil using $C_{12}A_7O^-$-based catalysts. *Appl. Catal. A: General* **2007**, *320*, 24-34.

(27) Wu, C.; Huang, Q.; Sui, M.; Yan, Y.; Wang, F. Hydrogen production via catalytic steam reforming of fast pyrolysis bio-oil in a two-stage fixed bed reactor system. *Fuel Process. Technol.* **2008**, *89*, 1306-1316.

(28) van Rossum, G.; Kersten, S.R.A.; van Swaaij, W.P.M. Staged catalytic gasification/steam reforming of pyrolysis oil. *Ind. Eng. Chem. Res.* **2009**, *48*, 5857-5866.

(29) Rioche, C.; Kulkarni, S.; Meunier, F.C.; Breen, J.P.; Burch, R. Steam reforming of model compounds and fast pyrolysis bio-oil on supported noble metal catalysts. *Appl. Catal. B: Environmental* **2005***, 61*, 130-139.

(30) Basagianis, A.C.; Verykios, X.E. Reforming reactions of acetic acid on nickel catalysts over a wide temperature range. *Appl. Catal. A: General* **2006**, *308*, 182-193.

(31) Bimbela, F.; Oliva, M.; Ruiz, J.; García, L.; Arauzo, J. Hydrogen production by catalytic steam reforming of acetic acid, a model compound of biomass pyrolysis liquids. *J. Anal. Appl. Pyrolysis* **2007**, *79*, 112-120.

(32) Bimbela, F.; Oliva, M.; Ruiz, J.; García, L.; Arauzo, J. Catalytic steam reforming of model compounds of biomass pyrolysis liquids in fixed bed: acetol and n-butanol. *J. Anal. Appl. Pyrolysis* **2009**, *85*, 204-213.

(33) Bimbela, F.; Chen, D.; Ruiz, J.; García, L.; Arauzo, J. Ni/Al co-precipitated catalysts modified with magnesium and copper for the catalytic steam reforming of model compounds from biomass pyrolysis liquids. *Appl. Catal. B: Environmental* **2012**, *119-120*, 1-12.

(34) Ramos, M.C.; Navascués, A. I.; García, L.; Bilbao, R. Hydrogen production by catalytic steam reforming of acetol, a model compound of bio-oil. *Ind. Eng. Chem. Res.* **2007**, *46*, 2399-2406.

(35) Medrano, J.A.; Oliva, M.; Ruiz, J.; García, L.; Arauzo, J. Catalytic steam reforming of model compounds of biomass pyrolysis liquids in fluidized bed reactor with modified Ni/Al catalysts. *Int. J. Hydrogen Energy.* **2009**, *85*, 214-225.

(36) Takanabe, K.; Aika, K.; Inazu, K.; Baba, T.; Seshan, K.; Lefferts, L. Steam reforming of acetic acid as a biomass derived oxygenate: Bifunctional pathway for hydrogen formation over Pt/ZrO_2 catalysts. *J. Catal.* **2006**, *243*, 263-269.

(37) Takanabe, K.; Aika, K.; Seshan, K.; Lefferts, L. Catalyst deactivation during steam reforming of acetic acid over Pt/ZrO_2. *Chem. Eng. J.* **2006**, *120*, 133-137.

(38) Czernik, S.; French, R.; Feik, C.; Chornet, E. Hydrogen by catalytic steam reforming of liquid byproducts from biomass thermoconversion processes. *Ind. Eng. Chem. Res.* **2002**, *41*, 4209-4215.

(39) Medrano, J.A.; Oliva, M.; Ruiz, J.; García, L.; Arauzo, J. Hydrogen from aqueous fraction of biomass pyrolysis liquids by catalytic steam reforming in fluidized bed. *Energy* **2011**, *36*, 2215-24.

(40) Li, H.; Xu, Q.; Xue, H.; Yan, Y. Catalytic reforming of the aqueous phase derived from Fast-pyrolysis of biomass. *Renew. Energy* **2009**, *34*, 2872-2877.

(41) Zhang, S.; Li, X.; Xu, Q.; Yan, Y. Hydrogen production from the aqueous phase derived from fast pyrolysis of biomass. *J. Anal. Appl. Pyrolysis* **2011**, *92*, 158-63.

(42) Remon, J.; Medrano, J.A.; Bimbela, F.; García, L.; Arauzo, J. Ni/Al-Mg-O solids modified with Co or Cu for the catalytic steam reforming of bio-oil. *Appl. Catal. B: Environmental* **2013**, *132-133*, 433-444.

(43) Xu, Q.; Lan, P.; Zhang, B.; Ren, Z.; Yan, Y. Hydrogen production via catalytic reforming of fast pyrolysis bio-oil in a fluidized-bed reactor. *Energy Fuels* **2010**, *24*, 6456-6462.

(44) Lan, P.; Xu, Q.; Zhou, M.; Lan, L.; Zhang, S.; Yan, S. Catalytic steam reforming of Fast pyrolysis bio-oil in fixed bed and fluidized bed reactors catalytic. *Chem. Eng. Technol.* **2010**, *33*, 2021-2028.

(45) Valle, B.; Remiro, A.; Olazar, M.; Bilbao, J.; Gayubo, A.G. Catalysts of $Ni/\alpha\text{-}Al_2O_3$ and $Ni/La_2O_3\text{-}\alpha Al_2O_3$ for hydrogen production by steam reforming of bio-oil aqueous fraction with pyrolytic lignin retention. *Int. J. Hydrogen Energy* **2013**, *38*, 1307-1318.

(46) Remiro, A; Valle, B.; Aguayo, A.T.; Bilbao, J.; Gayubo, A.G. Operating conditions for attenuating Ni/La_2O_3-αAl_2O_3 catalyst deactivation in the steam reforming of bio-oil aqueous fraction. *Fuel Process. Technol.* **2013**, *115*, 222-232.

(47) Yan, C.F.; Hu, E.Y.; Cai, C.L. Hydrogen production from bio-oil aqueous fraction with in situ carbon dioxide capture. *Int. J. Hydrogen Energy* **2010**, *35*, 2612-16.

(48) Chen, Z.; Song, H.S.; Portillo, M.; Lim, C.J.; Grace, J.R.; Anthony, E.J. Long-term calcinations/carbonation cycling and thermal pretreatment for CO_2 capture by limestone and dolomite. *Energy Fuels* **2009**, *23*, 1437-1444.

(49) Fernández-Akarregi, A. R.; Makibar, J.; López, G.; Amutio, M.; Olazar, M. Design and operation of a conical spouted bed reactor pilot plant (25 kg/h) for biomass fast pyrolysis. *Fuel Process. Technol.* **2013**, *112*, 48-56.

(50) Amutio, M.; Lopez, G.; Aguado, R.; Artetxe, M.; Bilbao, J.; Olazar, M. Kinetic study of lignocellulosic biomass oxidative pyrolysis. *Fuel* **2012**, *95*, 305-311.

(51) Amutio, M.; Lopez, G., Aguado, R.; Bilbao, J.; Olazar, M. Biomass oxidative flash pyrolysis: autothermal operation, yields and product properties. *Energy Fuels* **2012**, *26*, 1353-1362.

(52) Alberton. A.L.; Souza, M.M.V.M.; Schmal, M. Carbon formation and its influence on ethanol steam reforming over Ni/Al_2O_3 catalysts. *Catal. Today* **2007**, *123*, 257-264.

(53) Gayubo, A.G.; Valle, B.; Aguayo, A.T.; Olazar, M.; Bilbao, J. Pyrolytic lignin removal for the valorisation of biomass pyrolysis crude bio-oil by catalytic transformation, *J. Chem. Tech. Biotechnol.* **2010**, *85*, 132-144.

(54) Gayubo, A.G.; Valle, B.; Aguayo, A.T.; Olazar, M.; Bilbao, J. Olefin production by catalytic transformation of crude bio-oil in a two-step process. *Ind. Eng. Chem. Res.* **2010**, *49*, 123-131.

(55) Valle, B.; Gayubo, A.G.; Aguayo, A.T.; Olazar, M.; Bilbao, J. Selective production of aromatics by crude bio-oil valorization with a Ni modified HZSM-5 catalyst. *Energy Fuels* **2010**, *24*, 2060-2070.

(56) Galdámez, J.R.; García, L.; Bilbao, R. Hydrogen production by steam reforming of bio-oil using co-precipited NiAl catalysts. Acetic acid as a model compound. *Energy Fuels* **2005***, 19*, 1133-1142.

(57) Charitos, A.; Hawthorne, C.; Bidwe, A.R.; Sivalingam, S.; Schuster, A.; Spliethoff, H.; Scheffknecht, G. Parametric investigation of the calcium looping process for CO_2 capture in 10 kW_{th} dual fluidized bed. *Int. J. Greenhouse Gas control* **2010**, *4*, 776-784.

(58) Bauer, F.; Karge, H.G. Characterization of Coke on Zeolites in *Molecular Sieves*; Springer-Verlag: Berlin, Heidelberg, 2007.

(59) Ereña, J.; Sierra, I.; Olazar, M.; Gayubo, A.G.; Aguayo, A.T. Deactivation of a CuO-ZnO-Al_2O_3/γ-Al_2O_3 catalyst in the synthesis of dimethyl ether. *Ind. Eng. Chem. Res.* **2008**, *47*, 2238-2247.

(60) Sierra, I.; Ereña, J.; Aguayo, A.T.; Arandes, J.M.; Olazar, M.; Bilbao, J. Co-feeding water to attenuate deactivation of the catalyst metallic function ($CuO–ZnO–Al_2O_3$) by coke in the direct synthesis of dimethyl ether. *Appl. Catal. B: Environmental* **2011**, *106*, 167-173.

(61) Valle, B.; Castaño, P.; Olazar, M.; Bilbao, J.; Gayubo, A. G. Deactivating species in the transformation of crude bio-oil with methanol into hydrocarbons on a HZSM-5 catalyst. *J. Catal.* **2012**, *285*, 304–314.

(62) Wu, C.; Huang, Q.; Sui, M.; Yan, Y.; Wang, F. Hydrogen production via catalytic steam reforming of fast pyrolysis bio-oil in a two-stage fixed bed reactor system. *Fuel Process. Technol.* **2008**, *89*, 1306-1316.

(63) Chen, Z.; Grace, J.R.; Lim., C.J. CO_2 capture and hydrogen production in an integrated fluidized bed reformer-regenerator system. *Ind. Eng. Chem. Res.* **2011**, *50*, 4716-4721.

Figure Captions

Figure 1. Scheme of the reaction equipment.

Figure 2. Linkage between the steps of reforming, cracking and CO_2 capture in the catalyst/dolomite system.

Figure 3. Mass balance of oxygenates in both steps of the process.

Figure 4. Evolution with time on stream of bio-oil conversion and H_2 and CO_2 yields (a), CO, CH_4 and hydrocarbons yields (b). Reaction conditions: 600 ºC; S/C, 10; space-time, 2.8 $g_{dolomite}$ h $(g_{bio\text{-}oil})^{-1}$.

Figure 5. Comparison of reforming activity at different temperature of dolomite (solid lines) and inert CSi (dashed lines). (a) bio-oil conversion and H_2 and CO_2 yields; (b) CO, CH_4 and hydrocarbons yields. Reaction conditions: S/C, 10; space-time, 1.9 $g_{dolomite}$ h $(g_{bio\text{-}oil})^{-1}$.

Figure 6. Evolution with time on stream of bio-oil conversion and H_2 and CO_2 yields (a), CO, CH_4 and hydrocarbons yields (b). Reaction conditions: 600 ºC; S/C, 10; space-time, 0.45 $g_{catalyst}$ h $(g_{bio\text{-}oil})^{-1}$; dolomite mass, 1.3 g; catalyst/dolomite mass ratio, 0.38.

Figure 7. Effect of catalyst/dolomite mass ratio on bio-oil conversion and H_2 and CO_2 yiels (a), CO, CH_4 and hydrocarbons (b) under conditions of CO_2 capture (t= 0 h) and saturated dolomite (t= 4 h). Reaction conditions: 600 ºC; S/C, 10; space-time, 0.45 $g_{catalyst}$ h $(g_{bio\text{-}oil})^{-1}$.

Figure 8. Effect of catalyst/dolomite mass ratio on the evolution with time on stream of bio-oil conversion (a) and yields of H_2 (b), CO_2 (c), CO (d), CH_4 (e) and hydrocarbons (f). Reaction conditions: 600 ºC; S/C, 10; space time, 0.45 $g_{catalyst}$ h $(g_{bio\text{-}oil})^{-1}$.

Figure 9. Effect of dolomite mass on the evolution with time on stream of H_2 and CO_2 yields (a), CO and CH_4 yields (b). Reaction conditions: 600 ºC; S/C, 10; space-time, 0.45 and 1.35 $g_{catalyst}$ h $(g_{bio\text{-}oil})^{-1}$; catalyst/dolomite mass ratio, 0.38.

Figure 10. Effect of temperature on the evolution with time on stream of bio-oil conversion (a) and yields of H_2 (b), CO_2 (c), CO (d), CH_4 (e) and hydrocarbons (f). Reaction conditions: catalyst/dolomite mass ratio, 0.17; space-time, 0.45 $g_{catalyst}$ h $(g_{bio\text{-}oil})^{-1}$; S/C, 10.

Figure 11. Profiles of temperature-programmed-oxidation (TPO) analysis of the coke deposited on the catalyst (a) and on the dolomite (b) at different reaction temperatures.

Figure 12. Effect of S/C ratio on the evolution with time on stream of H_2 and CO_2 yields (a), CO and CH_4 yields (b). Reaction conditions: 600 ºC; catalyst/dolomite mass ratio, 0.17. space-time, 0.45 $g_{catalyst}$ h $(g_{bio\text{-}oil})^{-1}$.

TABLES

Table 1. Composition (wt%) of the raw bio-oil and its aqueous fraction.

Compound/Group	Raw bio-oil	Aqueous fraction
Acetic acid	12.8	19.1
Acetone	5.5	1.0
1-hydroxy-2-propanone	16.3	8.7
Hydroxyacetaldehyde	8.5	1.8
Methanol	1.3	1.0
Levoglucosan	11	19.6
Other ketones	3.8	8.1
Other acids	4.0	7.4
Other alcohols	2.4	3.6
Other aldehydes	6.5	5.5
Esters	5.1	3.1
Ethers	1.4	0.3
Phenols	16.6	13.4
Others	2.3	3.8
Non-identified	2.6	3.8

Table 2. Physical properties of dolomite.

Composition, wt%	
$CaCO_3$	58
$MgCO_3$	36
S	0.07
Fe_2O_3	0.3
Density, $g \cdot cm^{-3}$	2.8
Granulometry, mm	< 3

FIGURES

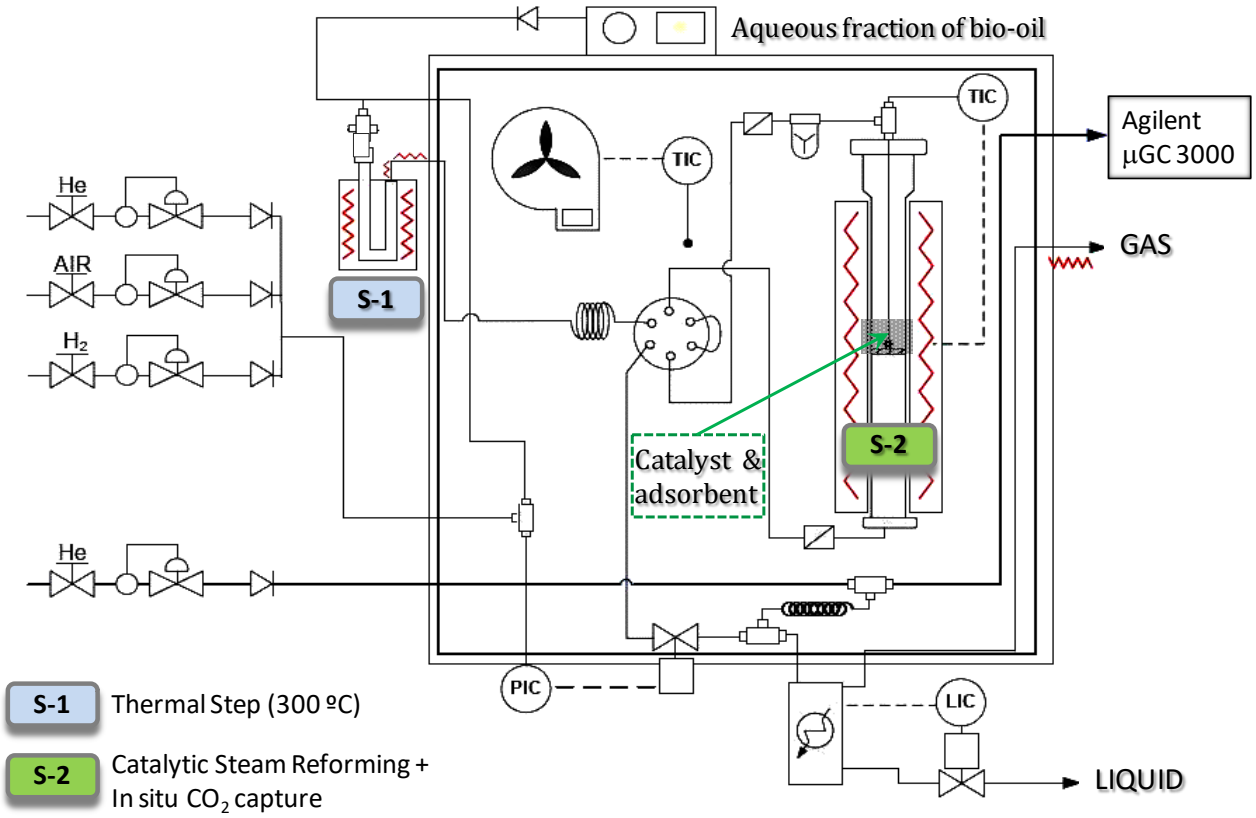

Figure 1

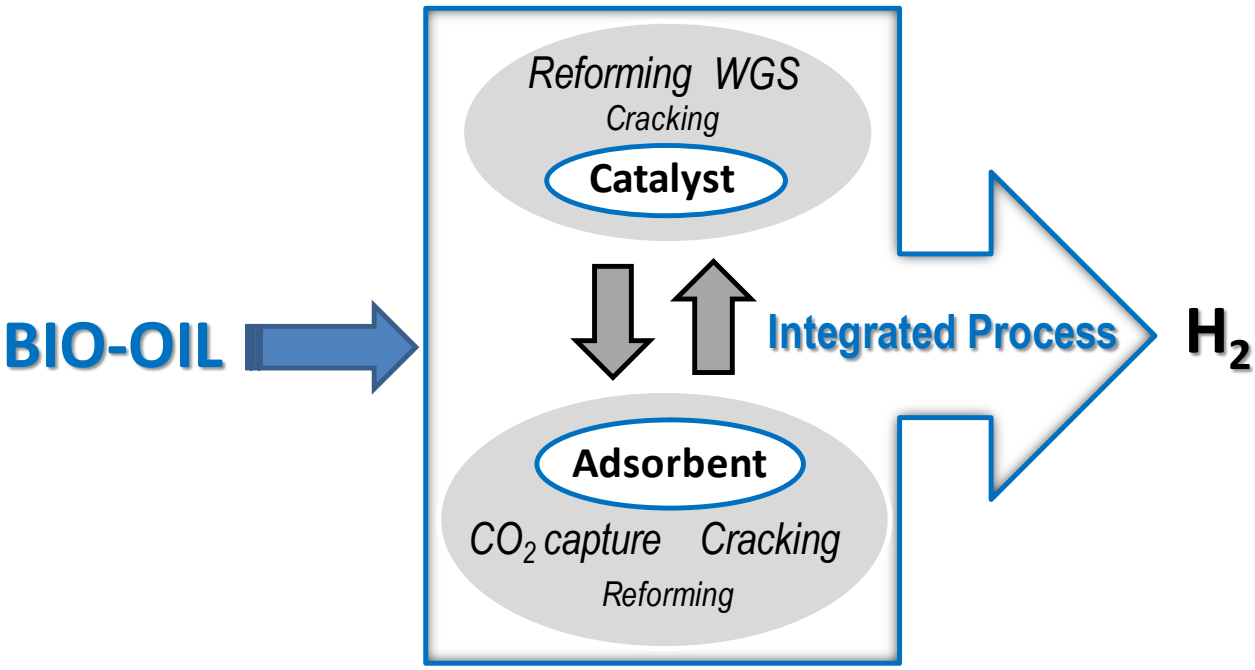
Reforming WGS
Cracking
Catalyst
BIO-OIL
Integrated Process
H2
Adsorbent
CO2 capture Cracking
Reforming

Figure 2

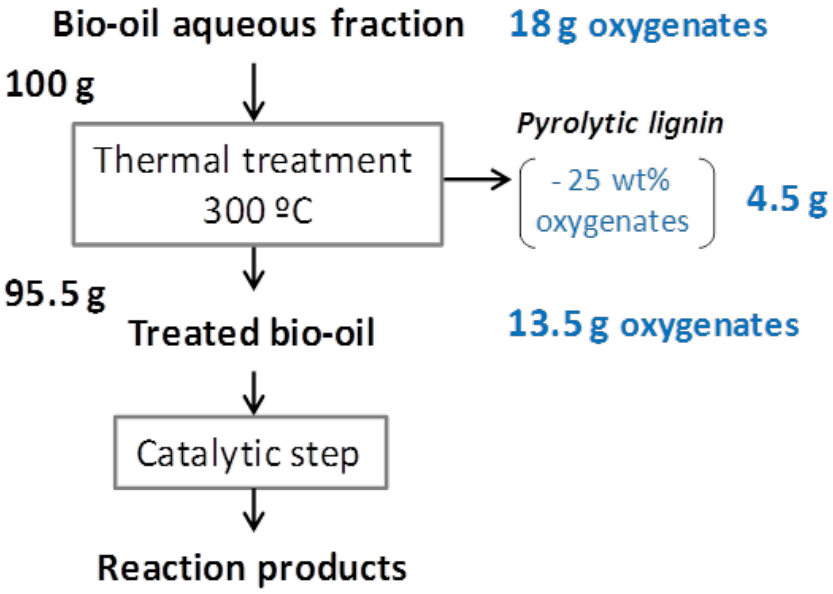
Bio-oil aqueous fraction
18 g oxygenates
100 g
Thermal treatment
300 ºC
Pyrolytic lignin
- 25 wt%
oxygenates
4.5 g
95.5 g
Treated bio-oil
13.5 g oxygenates
Catalytic step
Reaction products

Figure 3

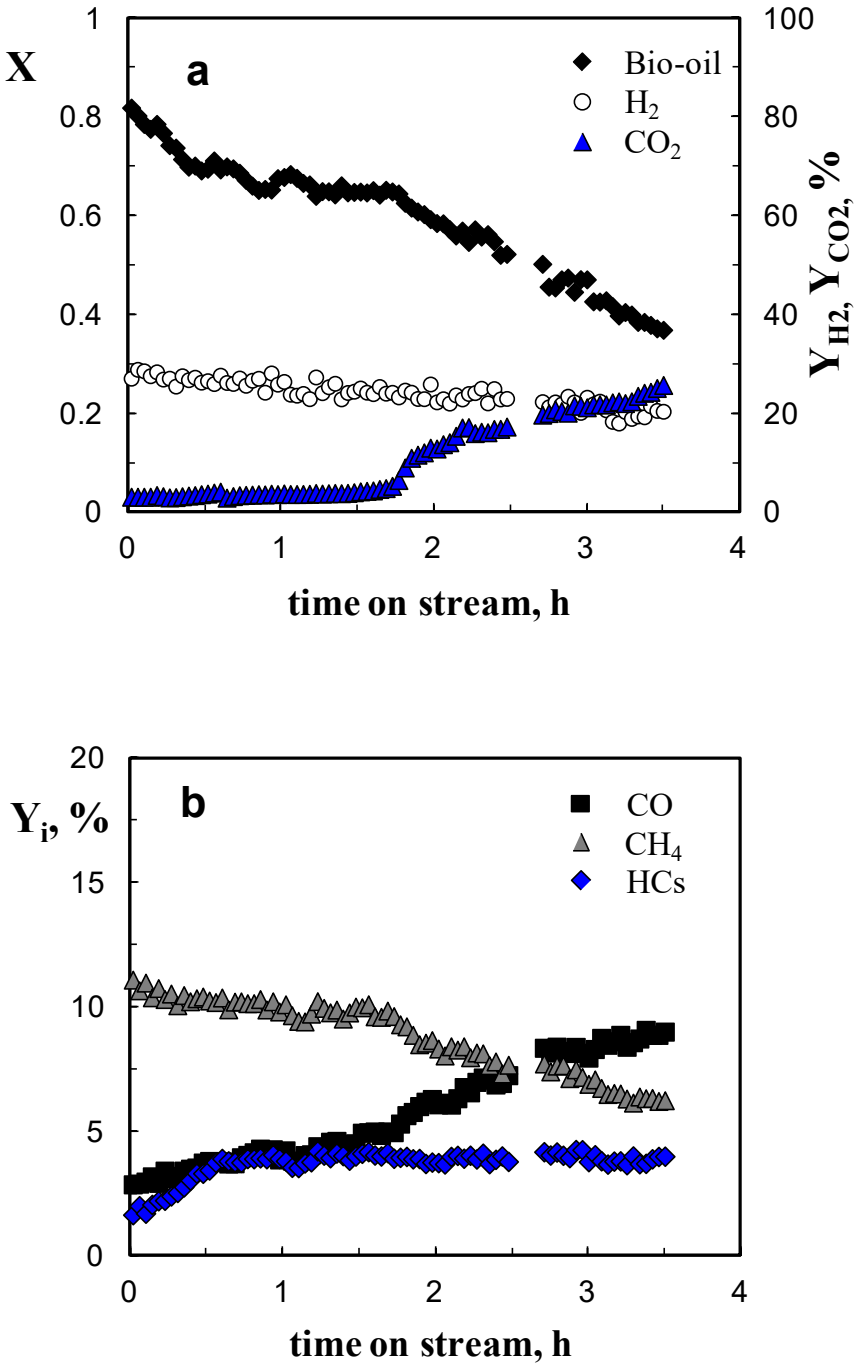
a
X
Bio-oil
H2
CO2
Y H2, Y CO2, %
time on stream, h
b
Yi, %
CO
CH4
HCs
time on stream, h

Figure 4

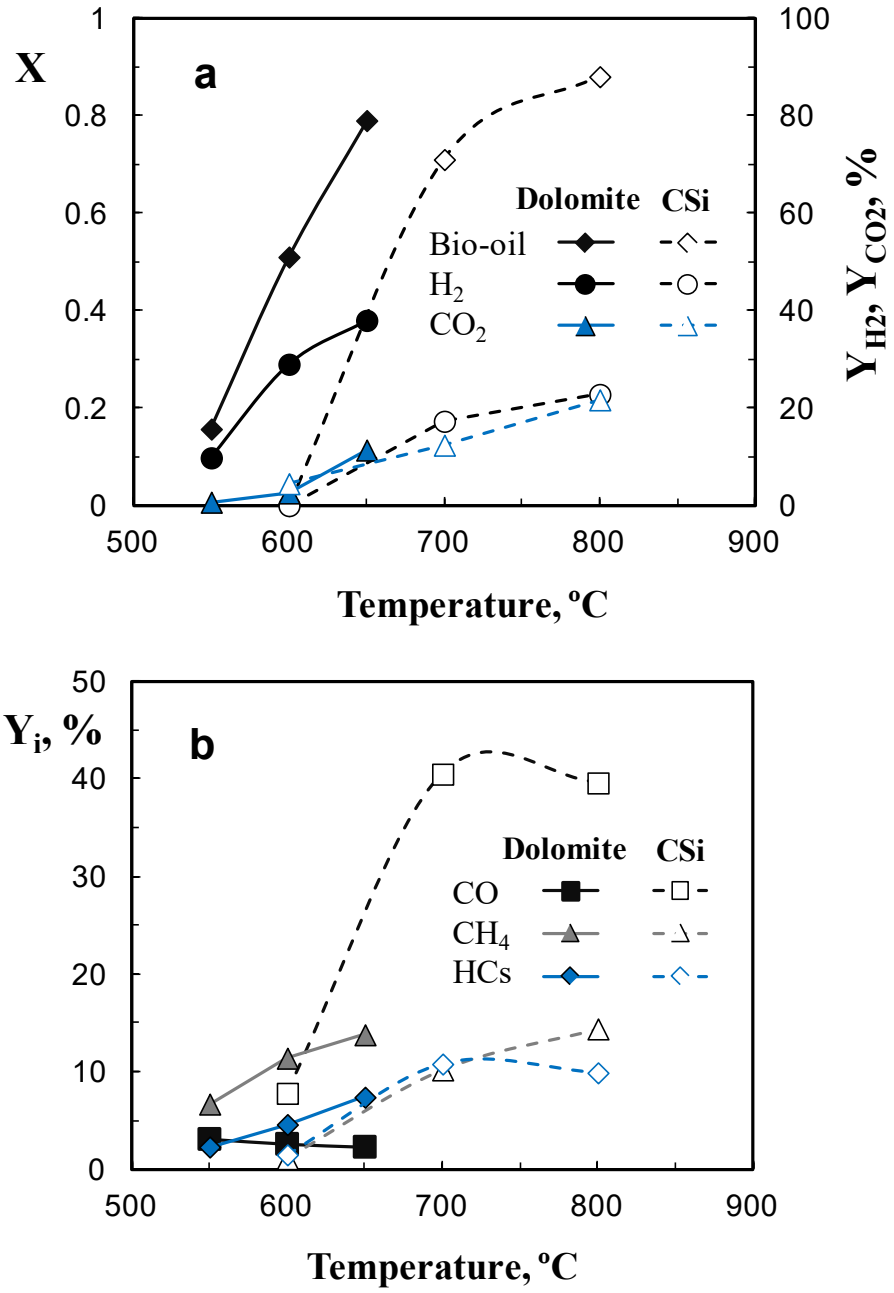
a
X
1
0.8
0.6
0.4
0.2
0
100
80
60
40
20
0
500
600
700
800
900
Temperature, ºC
Dolomite
CSi
Bio-oil
H2
CO2
YH2, YCO2, %
b
Yi, %
50
40
30
20
10
0
CO
CH4
HCs
Temperature, ºC

Figure 5

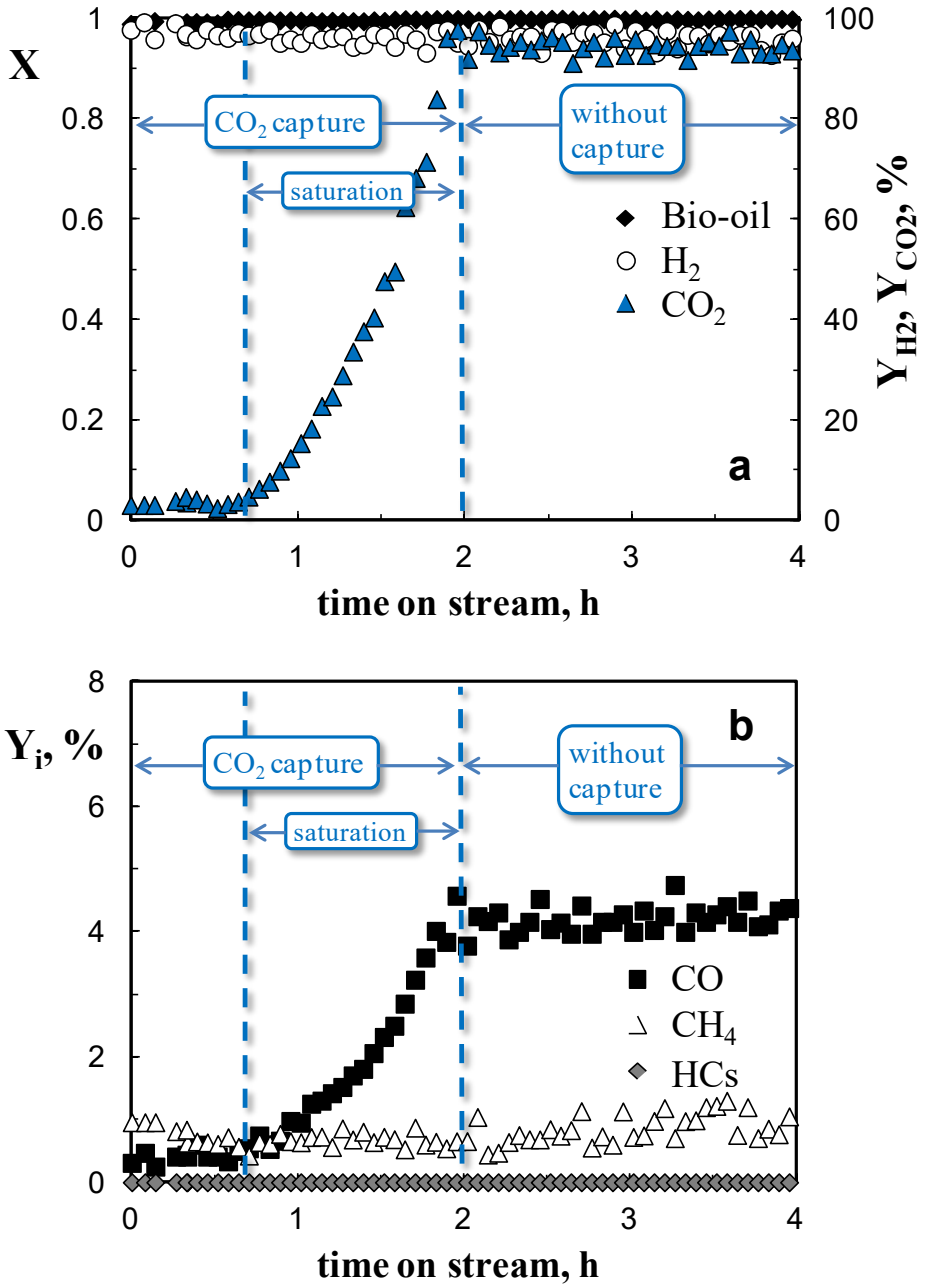
X
1
0.8
0.6
0.4
0.2
0
100
80
60
40
20
0
Y_{H2}, Y_{CO2}, %
CO_2 capture
without capture
saturation
Bio-oil
H_2
CO_2
a
0
1
2
3
4
time on stream, h
Y_i, %
8
6
4
2
0
b
CO_2 capture
without capture
saturation
CO
CH_4
HCs
0
1
2
3
4
time on stream, h

Figure 6

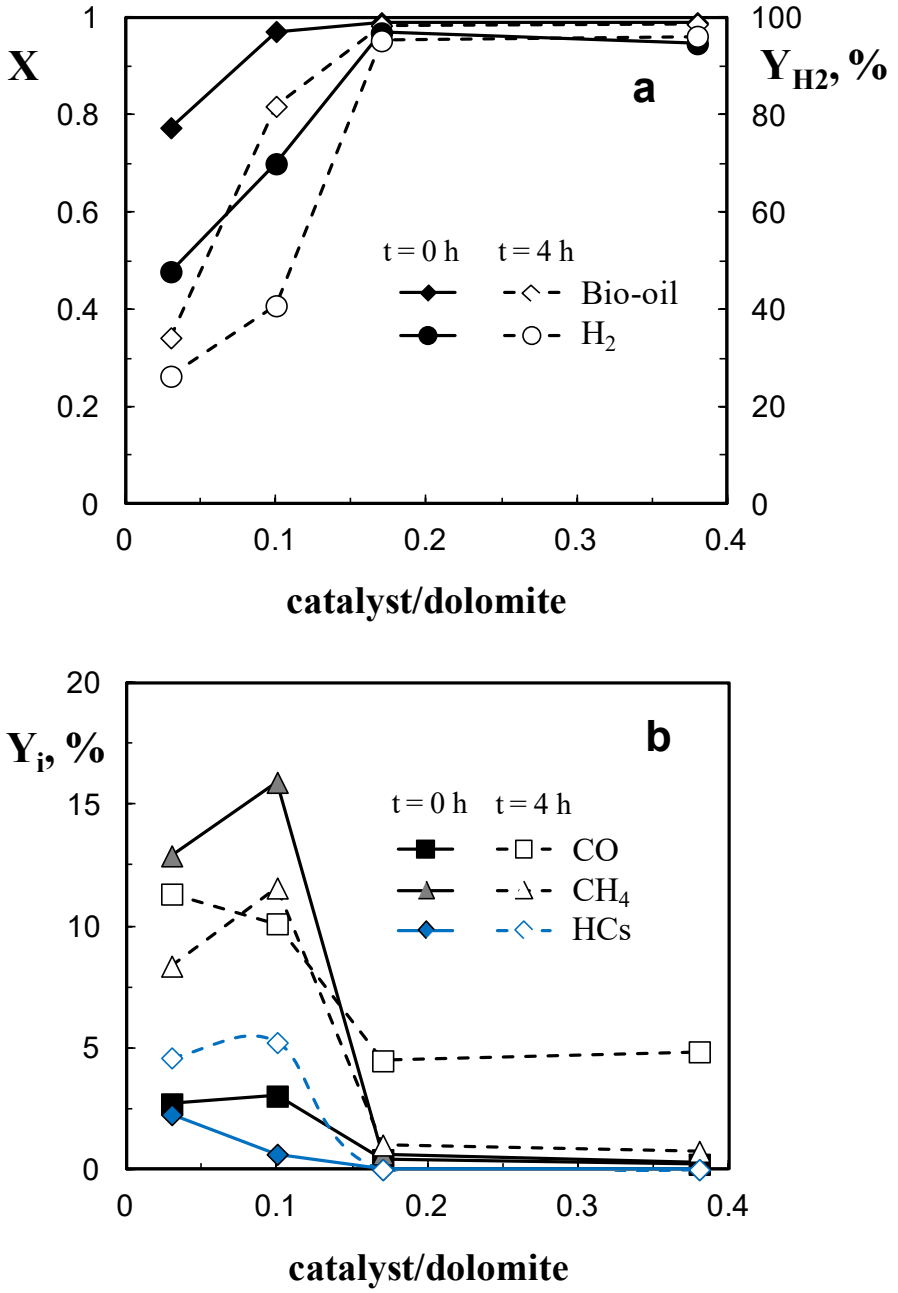
X
Y_{H2}, %
a
t = 0 h
t = 4 h
Bio-oil
H_2
catalyst/dolomite
Y_i, %
b
t = 0 h
t = 4 h
CO
CH_4
HCs
catalyst/dolomite

Figure 7

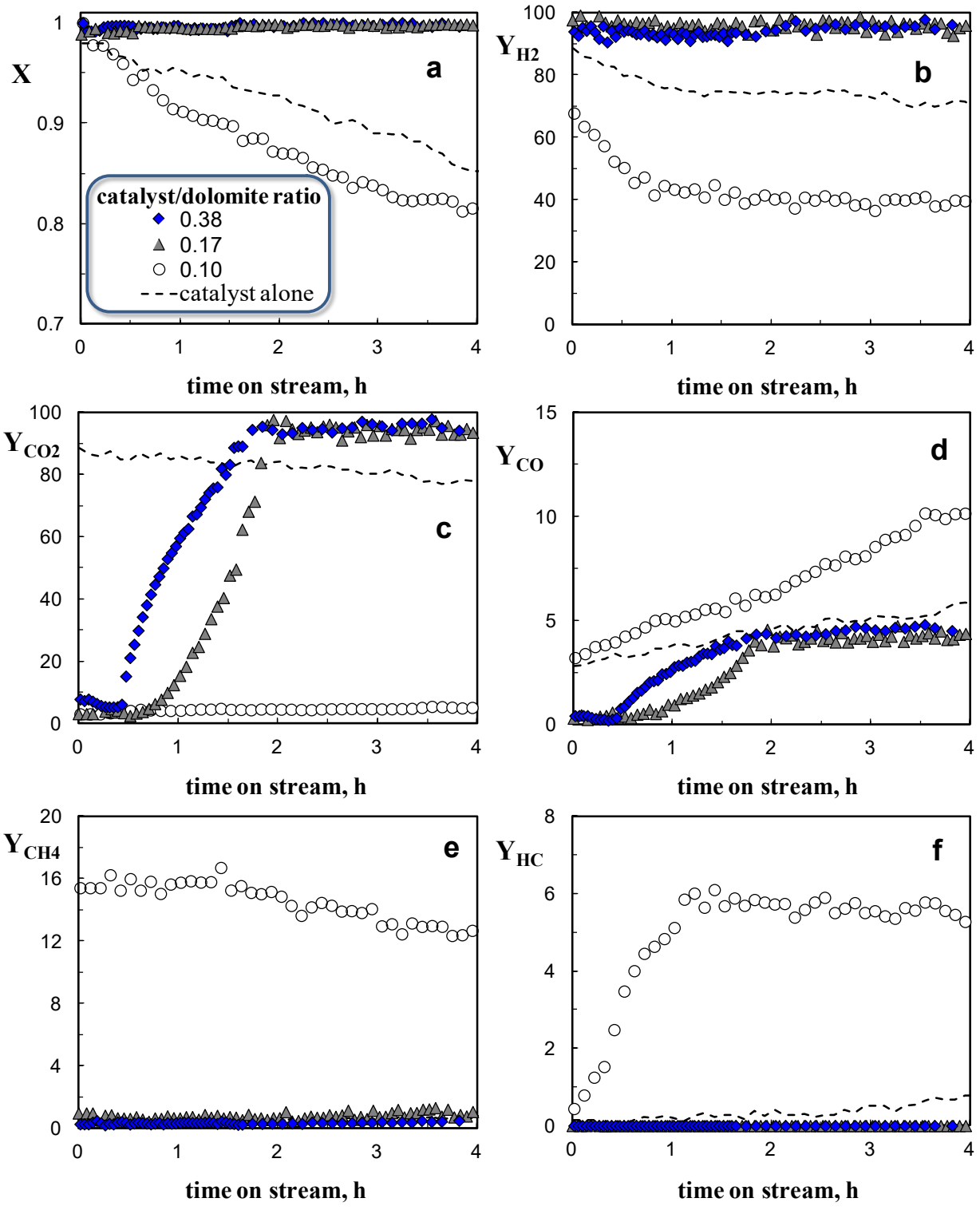
X
a
catalyst/dolomite ratio
0.38
0.17
0.10
catalyst alone
time on stream, h
Y_{H2}
b
time on stream, h
Y_{CO2}
c
time on stream, h
Y_{CO}
d
time on stream, h
Y_{CH4}
e
time on stream, h
Y_{HC}
f
time on stream, h

Figure 8

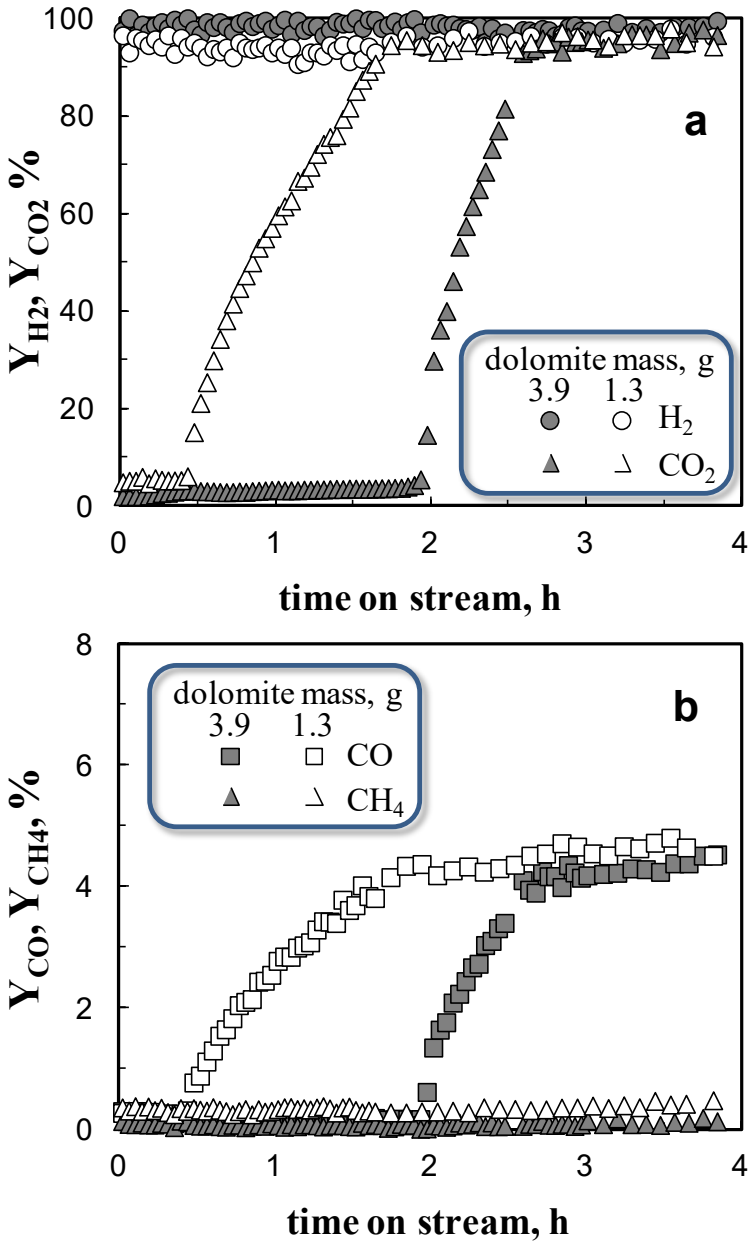
a
dolomite mass, g
3.9 1.3
H2
CO2
Y H2, Y CO2 %
time on stream, h
b
dolomite mass, g
3.9 1.3
CO
CH4
Y CO, Y CH4, %
time on stream, h

Figure 9

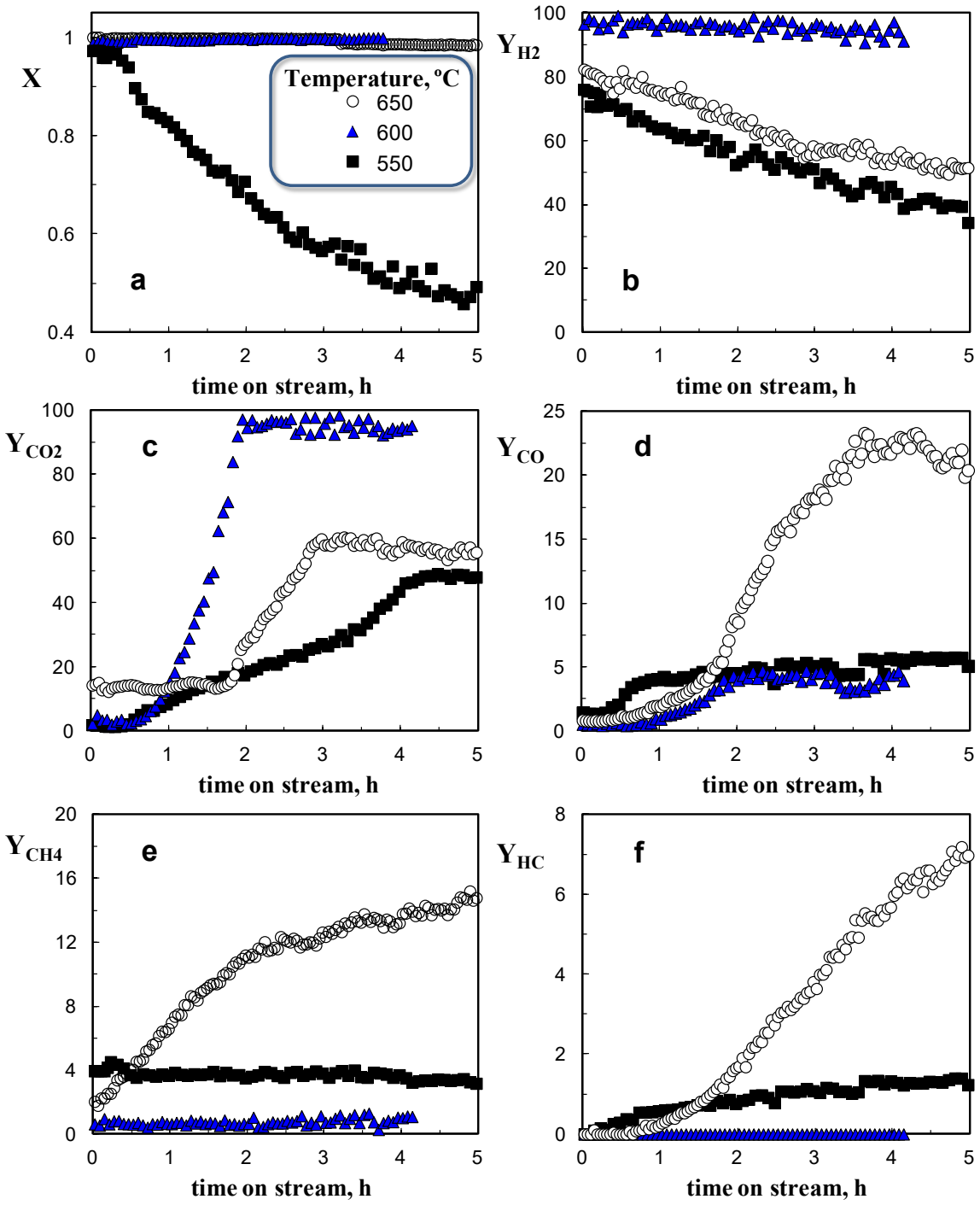
X
Temperature, °C
650
600
550
a
time on stream, h
Y_{H2}
b
time on stream, h
Y_{CO2}
c
time on stream, h
Y_{CO}
d
time on stream, h
Y_{CH4}
e
time on stream, h
Y_{HC}
f
time on stream, h

Figure 10

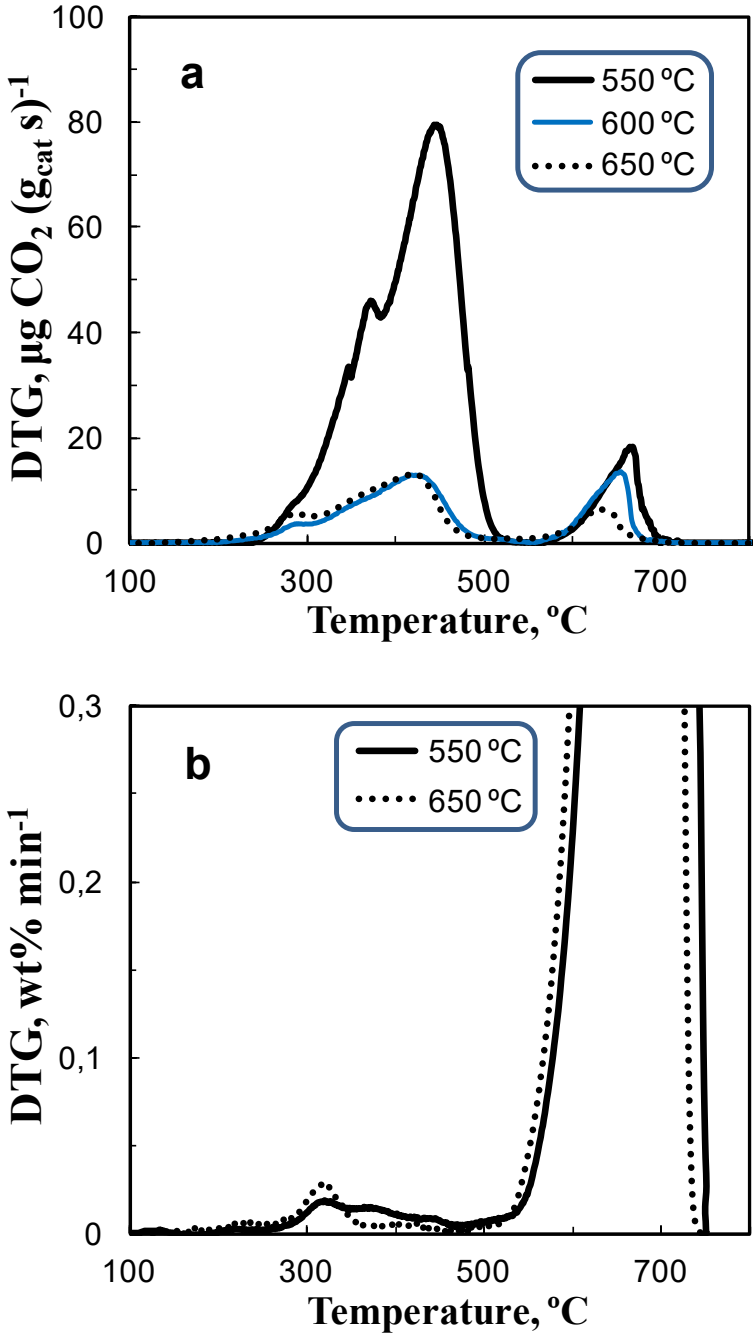
a
550 ºC
600 ºC
650 ºC
DTG, µg CO2 (gcat s)-1
100
80
60
40
20
0
100
300
500
700
Temperature, ºC
b
550 ºC
650 ºC
DTG, wt% min-1
0,3
0,2
0,1
0
100
300
500
700
Temperature, ºC

Figure 11

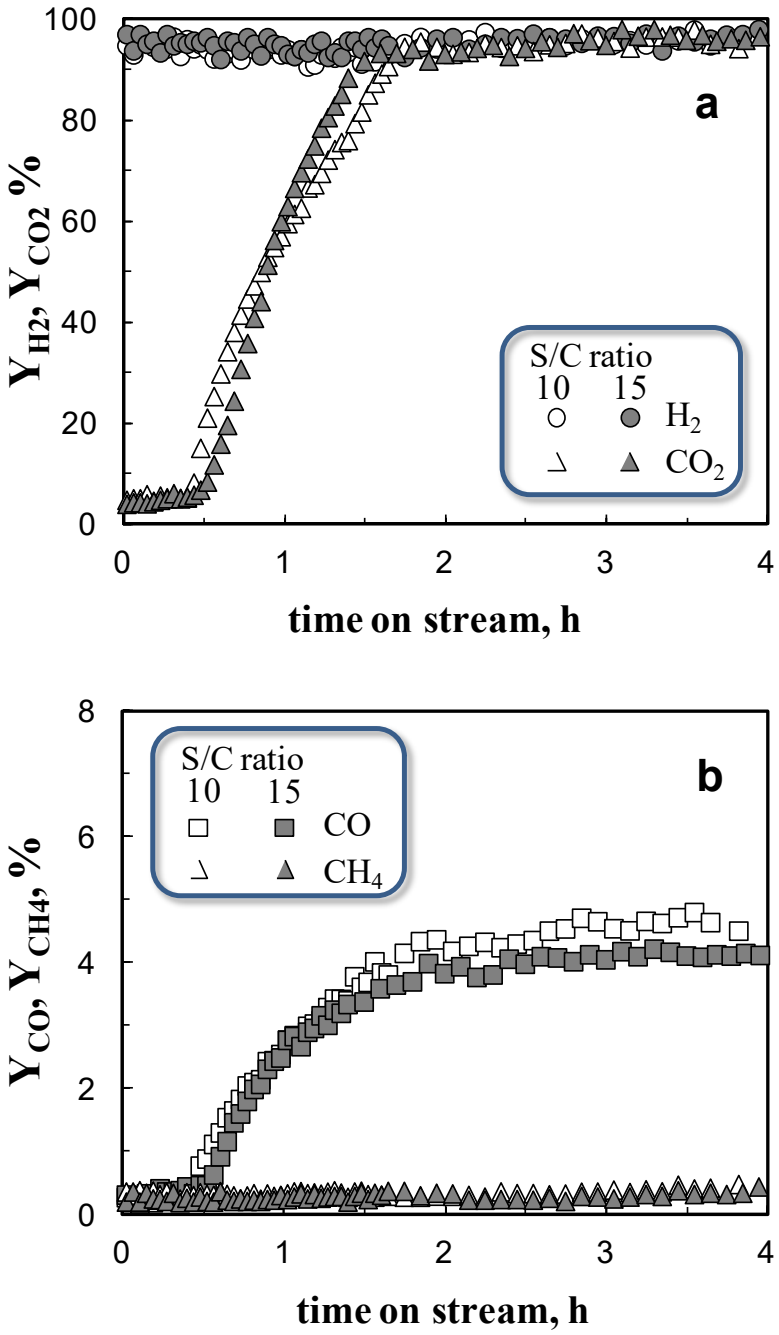
a
b
S/C ratio
10
15
H2
CO2
CO
CH4
Y H2, Y CO2 %
Y CO, Y CH4, %
time on stream, h
time on stream, h

Figure 12